Determination of $|V_{ub}|$ from inclusive semileptonic decay spectra

Boris Blok
Physics Department, Technion, Haifa, Israel

Thomas Mannel
Theory Division, CERN, CH-1211 Geneva 23, Switzerland

(Received 13 June 1994; revised manuscript received 5 August 1994)

We discuss the possibility of a model-independent method to determine $|V_{ub}|$ from appropriately constructed moments of the energy spectrum of the charged lepton in inclusive semileptonic B decays. The method includes perturbative QCD corrections as well as nonperturbative ones.

PACS number(s): 12.15.Hh, 12.39.Hg, 13.20.He

I. INTRODUCTION

Recently the inclusive decay spectra of heavy hadrons have attracted renewed attention. It has been shown that by a combination of heavy quark effective theory and the operator product expansion one may perform a systematic $1/m_Q$ expansion of the charged-lepton spectrum in inclusive heavy-hadron decays [1–9]. However, it turns out that an adequate description of the end-point region, where the charged-lepton energy $E_\ell \sim E_{\max}$, requires a partial resummation of the operator product expansion, yielding a result analogous to the leading-twist terms in deep inelastic scattering. In particular, it involves the analogue of the parton distribution function, which in the present case describes the end-point region of the lepton spectrum. While in most of the phase space the nonperturbative corrections may be described in terms of a few parameters, the end-point region needs the input of a nonperturbative function [10–12]. These recent ideas constitute a substantial conceptual progress towards a model-independent description of inclusive decay spectra, including the end-point region.

However, aside from the nonperturbative effects one has to include also QCD radiative corrections before one may confront the theory with data. These corrections have been calculated [13–17] and are known to be small for $b \to c$ transitions over the whole phase space. This is also true for the $b \to u$ case, as long as one is not too close to the end point $E_\ell \sim E_{\max}$. Neglecting the mass of the u quark one finds Sudakov-like double logarithms of the form $\ln^2(E_{\max} - E_\ell)$ as well as single logarithms $\ln(E_{\max} - E_\ell)$, indicating a breakdown of perturbation theory close to the end point.

In the present context the QCD radiative corrections have been studied by Falk *et al.* [18] and Bigi *et al.* [11]. Falk *et al.* arrive at the conclusion that the end-point region of the $b \to u$ decays is strongly affected by QCD radiative corrections and in principle a resummation to all orders becomes necessary. The conclusion of [18] is that the extraction of the nonperturbative effects becomes practically impossible due to large and mainly uncontrollable perturbative effects.

In [11] the Sudakov logarithms are exponentiated, leading to a strong modification of the end-point region. The authors of [11] suggest that uncontrollable radiative corrections discussed in [18] may be eliminated by the appropriate choice of the scale μ entering the strong coupling. They use $\mu \sim \sqrt{\Lambda m_b}$, where Λ is the characteristic momentum of light degrees of freedom in the heavy meson. However, this leads to a strong modification of the shape of the spectrum near the end point, and the reliability of the calculation becomes questionable.

Unfortunately, it is only the end-point region of charmless B decays that is not buried in the huge background of the charmed decays. The kinematic end point of the charmed B decays is $(m_B^2 - m_D^2)/(2m_B) \sim 2.3$ GeV, while for the charmless semileptonic decay it is $(m_B^2 - m_\pi^2)/(2m_B) \sim 2.6$ GeV. Hence there is only a window of at most 300 MeV, which may be attributed solely to the transition $b \to u\ell\nu$. The size of this window is of the order of the mass difference of the heavy meson and the heavy quark, $\bar\Lambda = m_B - m_b$, and thus it is not dominated by a few resonances. This would be the case in a smaller region of the size $\bar\Lambda(\bar\Lambda/m_b)$, which is of the order of tens of MeV, and in which the methods mentioned above would fail, since they are based on parton-hadron duality.

This paper is an attempt to define quantities which, on the one hand, are experimentally accessible and, on the other hand, allow us to disentangle perturbative and nonperturbative effects. Our suggestion is to calculate appropriate moments $\mathcal{M}_n$ of the measured spectrum, which are defined in such a way that they allow an expansion in both $\alpha_s(m_b)$ and $\bar\Lambda/m_b$, at least for some range of indices n.

Similar ideas have previously been put forward in [10, 11]. However, in these papers there was no detailed numerical study of such moments, including both radiative and nonperturbative effects.

In the next section we shall reconsider the perturbative and nonperturbative contributions to the decay spectrum of inclusive semileptonic charmless B decays and give the definition of the moments. In Sec. III, we perform a numerical study from which we obtain constraints on the range of the index n of the moments. Finally we give our conclusions and comment on the extraction of V_{ub}.

II. PERTURBATIVE AND NONPERTURBATIVE CONTRIBUTIONS TO THE SPECTRUM

It has been shown in [1–9] that one may obtain a systematic $1/m_b$ expansion for inclusive decay rates and the corresponding spectra. The leading term in this expansion is the free-quark decay, and the first nonvanishing corrections appear formally at order $1/m_b^2$. These are genuinely nonperturbative corrections, which are given in terms of two matrix elements

$$\langle B(v)|\bar{h}_v(iD)^2 h_v|B(v)\rangle = 2m_B\lambda_1, \tag{1}$$

$$\langle B(v)|\bar{h}_v(-i)\sigma_{\mu\nu}(iD^\mu)(iD^\nu)h_v|B(v)\rangle = 6m_B\lambda_2. \tag{2}$$

The parameter λ_2 is given in terms of the $0^- - 1^-$ mass splitting $\lambda_2 = (m_{B^*}^2 - m_B^2)/4 \sim 0.12$ GeV^2. The matrix element λ_1 is not as easily accessible, in particular it has not yet been determined experimentally. The theoretical estimates vary over a broad range [19, 20] of about $\lambda_1 \sim -(0.3-0.6)$ GeV^2; thus we shall consider below a typical "small" value $\lambda_1 = -0.3$ GeV^2 and a "large" one, $\lambda_1 = -0.6$ GeV^2.

The result for the spectrum of the inclusive decay $B \to X_u \ell\nu$, neglecting the mass of the u quark, is given by

$$\begin{aligned}\frac{1}{\Gamma_b}\frac{d\Gamma}{dy} = &\left[2y^2(3-2y) + \frac{10y^3}{3}\frac{\lambda_1}{m_b^2} + 2y^2(6+5y)\frac{\lambda_2}{m_b^2}\right] \\ &\times\Theta(1-y) - \frac{\lambda_1 + 33\lambda_2}{3m_b^2}\delta(1-y) \\ &-\frac{\lambda_1}{3m_b^2}\delta'(1-y),\end{aligned} \tag{3}$$

where

$$y = \frac{2E_\ell}{m_b} \quad \text{and} \quad \Gamma_b = \frac{G_F^2|V_{ub}|^2}{192\pi^3}m_b^5. \tag{4}$$

The δ-function singularities at the parton-model end point $y = 1$ indicate a breakdown of the operator product expansion. In fact, it has been pointed out in [4–6] that, for the decay spectra, the expansion parameter is in fact $\bar{\Lambda}/[m_b(1-y)]$, which becomes large close to the end point. Still these terms have an interpretation as being the first few terms of a moment expansion of a nonperturbative function describing the behavior of the spectrum close to the end point [10–12]:

$$\begin{aligned}\frac{d\Gamma}{dy} &= \Gamma_b\left[2\Theta(1-y) + \sum_{n=1}^{\infty}\frac{a_n}{m_Q^n}\frac{1}{n!}\delta^{(n-1)}(1-y)\right] \\ &= 2\Gamma_b\int_{(y-1)m_b/\bar{\Lambda}}^{1} F(x)dx,\end{aligned} \tag{5}$$

where $\delta^{(k)}$ denotes the kth derivative of the δ function. Note that a_1 vanishes and a_2 may be read off from (3) to be $a_2 = -2\lambda_1/3$.

The function $F(x)$ may be written formally as

$$F(x) = \frac{1}{2m_B}\left\langle B(v)|\bar{h}_v\delta\left(x - \frac{iD_+}{\bar{\Lambda}}\right)h_v|B(v)\right\rangle, \tag{6}$$

where $D_+ = nD, n^2 = 0, n_0 > 0$ is the positive light cone component of the covariant derivative and $\bar{\Lambda} = m_B - m_b$,

where $D_+ = nD, n^2 = 0, n_0 > 0$ is the positive light cone component of the covariant derivative and $\bar{\Lambda} = m_B - m_b$,
where m_B is the mass of the B meson. This function has support only in a region of $x \sim 1$. In particular, the function F leads to some "smearing" of the end-point region, with the effect that the end point of the spectrum is shifted from the parton-model end point $m_b/2$ to the physical end point $m_B/2$. Below we shall use some model input for F to estimate the size of the higher-order corrections close to the end point.

Aside from these nonperturbative corrections, there are also perturbative ones, which have been calculated some time ago. The order-α_s corrections are known for all values of the lepton energy [13–17]; however, since we are interested only in the behavior close to the end point, we shall consider here only the contributions relevant in this region. It turns out that the order-α_s corrections exhibit doubly and singly logarithmic divergences at the end point. Up to terms vanishing at the end point, the result reads [17]

$$\begin{aligned}\frac{d\Gamma}{dy} = \frac{d\Gamma^{(0)}}{dy}\Bigg[1 - \frac{2\alpha_s}{3\pi}[&\ln^2(1-y) \\ &+ \tfrac{31}{6}\ln(1-y) + \tfrac{5}{4} + \pi^2]\Bigg],\end{aligned} \tag{7}$$

where at the end point

$$\frac{1}{\Gamma_b}\frac{d\Gamma^{(0)}}{dy} = 2y^2(3-2y)\Theta(1-y) \to 2\Theta(1-y). \tag{8}$$

The scale μ of the strong coupling is not yet fixed in this expression; any scale choice will formally only affect subleading terms. However, from physical considerations one may be led to choose $\mu^2 \sim m_b^2(1-y)$, as was done in [11],[1] leading to an even more singular behavior with $y \to 1$. In any case, a resummation of the singular terms becomes mandatory in order to describe the spectrum close to the end point.

The common folklore is that the doubly logarithmic terms in (7) exponentiate, and at the level of the Sudakov logarithms the radiative corrections become

$$\frac{d\Gamma}{dy} = \frac{d\Gamma^{(0)}}{dy}\exp\left[-\frac{2\alpha_s}{3\pi}\ln^2(1-y)\right]. \tag{9}$$

Again the problem arises of the scale of α_s and we shall compare below two choices. Using the one-loop expression for α_s,

$$\alpha_s(\mu) = \frac{12\pi}{(33-2n_f)\ln(\mu^2/\Lambda_{\rm QCD}^2)}, \tag{10}$$

we will compare the results obtained for $\mu^2 = m_b^2$ and $\mu^2 \sim m_b^2(1-y)$, the latter expression leading to

[1] Actually, the scale chosen in [11] is $\mu^2 \sim \bar{\Lambda}m_b$, but this is equivalent to $\mu^2 \sim m_b^2(1-y)$, since in the end-point region $1-y \sim \bar{\Lambda}/m_b$.

$$\frac{d\Gamma}{dy} = \frac{d\Gamma^{(0)}}{dy} \exp\left[-\frac{8}{25}\frac{\ln^2(1-y)}{\ln[(m_b^2/\Lambda_{\rm QCD}^2)(1-y)]}\right]. \qquad (11)$$

In the end-point region one obtains qualitatively a behavior of the form [11]

$$\frac{d\Gamma}{dy} \sim \frac{d\Gamma^{(0)}}{dy}(1-y)^{(\epsilon_0-1)}, \qquad (12)$$

where

$$\epsilon_0 - 1 = -\frac{8}{25}\frac{\ln(1-y)}{\ln[(m_b^2/\Lambda_{\rm QCD}^2)(1-y)]}$$

behaves approximately like a constant in the region of interest [11].[2] However, after such a resummation to all orders of perturbation theory, it is no longer obvious how to disentangle perturbative from nonperturbative contributions. This becomes clear if one really treats ϵ_0 as a constant, in which case one may rewrite (12):

$$\frac{d\Gamma}{dy} \sim \frac{d\Gamma^{(0)}}{dy}\text{const} \times \exp\left\{\frac{12\pi(\epsilon_0-1)}{25} \times \frac{1}{\alpha_s[(m_b^2/\Lambda_{\rm QCD}^2)(1-y)]}\right\}, \qquad (13)$$

which in this form looks like a nonperturbative contribution.

The above discussion shows that the end-point region is in fact difficult to describe. On the one hand there are large nonperturbative contributions, on the other hand there are perturbative contributions, becoming large in the end-point region. These remarks, however, apply only to the spectrum itself. It has already been shown in [10, 11] that it may be helpful to consider appropriately defined moments of the spectrum, e.g., those taken with respect to the parton-model end point are related to the coefficients of the most singular δ-function-like singularities at the end point, in each order in the $1/m_b$ expansion.

Here we propose to consider a slightly different set of moments: namely,

$$\mathcal{M}_n = \int_0^{1+\bar\Lambda/m_b} dy\, y^n \frac{d\Gamma}{dy}, \qquad (14)$$

which may be rewritten in terms of the moments as defined in [10]. As we shall discuss in detail below, these moments have, for some range of n, a simultaneous expansion in $\alpha_s(m_b)$ and $\bar\Lambda/m_b$.

This range of n is specified by two requirements. Experimental information will be available only close to the end-point region, and thus n has to be large enough to be sensitive to this region. On the other hand, the larger n, the stronger the sensitivity to the details of the end-point region. In other words, only for not too large n may one perform the simultaneous perturbative and nonperturbative expansion; the problems present in the spectrum will reappear in the behavior of the moments $\mathcal{M}_n$ for large n.

In fact, from order-of-magnitude considerations one would expect that there is no such range in n, where n is large enough to be sensitive to the end point, and in which nonperturbative and radiative effects still remain under control. However, it turns out from the more detailed study presented below that there might be such a window in n.

In the next section we shall perform a numerical study for the radiative corrections and the nonperturbative contributions, in order to find a range in n where one may reliably calculate the moments $\mathcal{M}_n$.

III. NUMERICAL DISCUSSION

We shall first consider the moments of the differential distribution in the naïve parton model, without any corrections. The spectrum is given by the parton-model expression and one obtains, for the moments to zeroth order,

$$\mathcal{M}_n^{(0)} = \Gamma_b \frac{2(n+6)}{(n+3)(n+4)}. \qquad (15)$$

However, we are mainly interested in the end-point region, where the parton-model spectrum may be approximated by (8), and the moments obtained in this approximation are

$$\tilde{\mathcal{M}}_n^{(0)} = \Gamma_b \frac{2}{n+1}. \qquad (16)$$

In Fig. 1 we plot the moments obtained from the full parton-model rate versus the approximation (16). The comparison between the two sets gives some impression of the value of n at which there is sensitivity only to the end-point region; from the figure one reads off that already at $n \sim 4$ one mainly obtains information on the end point.

On the other hand, data will be available in the near future only for lepton energies above 2.3 GeV. Thus we

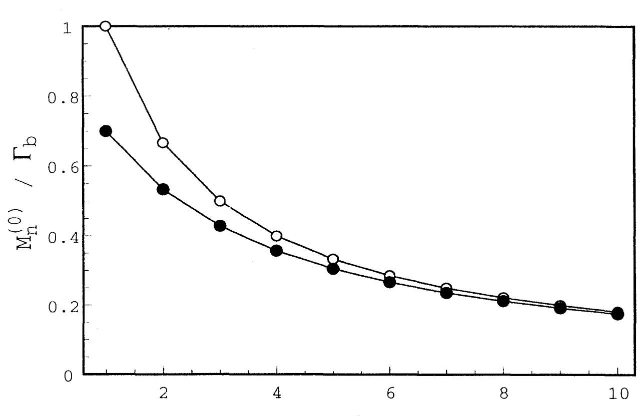

FIG. 1. Comparison of the parton model moments for the full y dependence (solid dots) vs the end-point approximation (8) (open circles).

---

[2]This is, however, a very rough approximation; between $y = 0.9$ and $y = 0.98$ $(\epsilon_0 - 1)$ varies between 0.2 and 0.6.

shall in the following consider also moments in which the integration over n is restricted to a range $y_0 < y < 1 + \bar{\Lambda}/m_b$:

$$\mathcal{M}_n(y_0) = \int_{y_0}^{1+\bar{\Lambda}/m_b} dy\, y^n \frac{d\Gamma}{dy}, \tag{17}$$

where realistic values for y_0 will be in the region of $y_0 = 0.9$ or even higher. Introducing such a lower cut will change (16) to

$$\tilde{\mathcal{M}}_n^{(0)} = \Gamma_b \frac{2}{n+1}\left(1 - y_0^{n+1}\right), \tag{18}$$

from which we estimate that the sixth moment will receive about 52% for $y_0 = 0.9$, the tenth moment already about 70% contribution from the region $y_0 < y < 1$, at least in the naïve parton model. For even higher values, say $y_0 = 0.95$, the sensitivity to the end-point region becomes less; in this case the tenth moment still has 43% contribution from this region. On the other hand, an upper limit of n is given by the experimental resolution. If data on $b \to u$ semileptonic transitions are available only in the small window between 2.3 GeV and 2.6 GeV, not enough data may be expected to extract moments higher than about $n = 10$. In what follows we shall thus concentrate on moments with n less than 10.

Next we turn to the nonperturbative corrections. They have been been given in (3) to order $1/m_Q^2$. Taking the moments of (3) one obtains, in the end-point approximation (8),

$$\mathcal{M}_n = \tilde{\mathcal{M}}_n^{(0)} + \Gamma_b\left[\frac{\lambda_1}{3m_b^2}\left(\frac{10}{n+1} - 1 - n\right) + \frac{\lambda_2}{m_b^2}\left(\frac{22}{n+1} - 11\right)\right]. \tag{19}$$

The dependence on n of the various terms in $\mathcal{M}_n$ reflects how singular the contribution is at the end point of the lepton spectrum. The most singular term is the one with the derivative of the δ function; this leads to a linear dependence in n. The terms behaving like a δ function yield constant terms in the moments, while terms with step functions will decrease as $1/n$ if n becomes large.

In a similar way as for the parton model we may estimate the effects of a lower cut off y_0 according to (17). For the terms involving a step function, the result is qualitatively the same as for the parton model, while for the contributions with δ-function-like singularities there is no dependence on the lower cut, since these are concentrated at $y = 1$.

Higher moments will become more and more sensitive to what happens in the end-point region. Thus (19) is not valid for n becoming too large. In order to estimate the value of n, where the expansion breaks down, we have to consider an even more singular contribution. This is contained in the next order of the $1/m_Q$ expansion, and has the form

$$\frac{d\Gamma}{dy} \sim \frac{a_3}{m_b^3}\delta''(1-y). \tag{20}$$

Here the parameter a_3 is related to the matrix element $\langle B(v)|\bar{h}_v(iD_\mu)(ivD)(iD^\mu)h_v|B(v)\rangle$, whose moment gives a contribution quadratic in n:

$$M_n \sim \Gamma_b n(n-1)\frac{a_3}{m_b^3}. \tag{21}$$

Neglecting the higher orders in the $1/m_Q$ expansion of the moments is only justified if

$$n(n-1)\frac{a_3}{m_b^3} < n\frac{3|\lambda_1|}{m_b^2} \quad \text{or } n < \frac{|\lambda_1| m_b}{3a_3} + 1. \tag{22}$$

Depending on the values of $|\lambda_1|$ and a_3 this limit ranges between 4 (for $a_3^{1/3} = |\lambda_1|^{1/2} = 500$ MeV) and 10 (for $a_3^{1/3} = 350$ MeV, $|\lambda_1|^{1/2} = 500$ MeV). Consequently, it depends on the size of the coefficients of the higher-order terms, whether one may obtain moments sufficiently high to be sensitive to the end point.

In order to estimate this one has to perform a resummation of the most singular terms at the end point, to all orders in $1/m_Q$; in other words one has to include these effects using the nonperturbative function $F(x)$ defined in (6). In terms of this the rate is given by (5), which describes the behavior of the lepton spectrum close to the end point, namely over a region of the order of $1 - y \sim \sqrt{|\lambda_1|}/m_b$. There is, however, an even smaller region $1 - y \sim (\sqrt{|\lambda_1|}/m_b)^2$, the resonance region, in which only a few resonances contribute to the spectrum. This region will start to contribute significantly to the moments for

$$n \sim \left(\frac{m_b}{\sqrt{|\lambda_1|}}\right)^2 \sim 100, \tag{23}$$

which means that moments with $n > 100$ will be determined from the contributions of only very few light resonances.

The function F is genuinely nonperturbative and it has been considered using several models. One frequently used model is the one of Altarelli *et al.* [15], which has been rewritten in terms of the nonperturbative function $F(x)$ [21] given by

$$F(x) = \frac{\bar{\Lambda}}{\sqrt{\pi}\, p_F}\exp\left(-\frac{1}{4}\left(\frac{p_F\rho}{\bar{\Lambda}(1-x)} - \frac{\bar{\Lambda}}{p_F}(1-x)\right)^2\right). \tag{24}$$

Here $\bar{\Lambda} = m_B - m_b$, and p_F is the so-called Fermi momentum, which corresponds to the motion of the heavy quark inside the heavy meson; see [21] for a precise definition. Finally, ρ is implicitly given in terms of the other two parameters by

$$\bar{\Lambda} = \frac{p_F\rho e^{(\rho/2)}K_1(\rho/2)}{\sqrt{\pi}}, \tag{25}$$

where K_1 is a modified Bessel function.

The model, as given in [21], has only one parameter ρ which has a physical interpretation, namely, $\rho = m_{\text{spectator}}^2/p_F^2$. One may also relate the model parameters to the QCD matrix element λ_1, since appropriate moments of F are related to matrix elements of powers of covariant derivatives between heavy-meson states. In this way one obtains the relation

$$1-\frac{\lambda_1}{3\bar{\Lambda}^2}=\pi\frac{2+\rho}{\rho^2 K_1^2(\rho/2)}e^{-\rho}, \tag{26}$$

which may be used to determine the value of the model parameter ρ in terms of $\bar{\Lambda}$ and λ_1; it has been pointed out in [21] that only the combination $\xi = -\lambda_1/(3\bar{\Lambda}^2)$ enters the model. In particular, Eq. (26) has no solution if ξ is larger than 0.57. For a value of $\bar{\Lambda}$ of 500 MeV, this means that the model cannot accommodate a value $-\lambda_1$ of more than 0.42 GeV^2. For this value we have $\rho = 0$, and the nonperturbative function simplifies

$$F(x)=\frac{2}{\pi}\exp\left(-\frac{(1-x)^2}{\pi}\right). \tag{27}$$

We shall use this model to estimate the effects of the most singular terms occurring in higher orders in the $1/m_b$ expansion.

The value of λ_1 is not yet known accurately. We shall consider below a "small" value, $\lambda_1 = -0.3$ GeV^2, as well as the largest value possible in the above model, $\lambda_1 = -0.43$ GeV^2. The first value of λ_1 corresponds to $\rho = 0.35$, while the large one is the limiting case $\rho = 0$. In our final result we shall also consider a "large" value $\lambda_1 = -0.6$ GeV^2. Furthermore, we will use $m_b = 4.78$ GeV and $\bar{\Lambda} \sim 500$ MeV in the following numerical analysis.

In Fig. 2 we plot the nonperturbative corrections $\delta\mathcal{M}_n^{(\mathrm{np})}$ to the moments, $\delta\mathcal{M}_n^{(np)} = \mathcal{M}_n^{(np)} - \tilde{\mathcal{M}}_n^{(0)}$. The upper plot corresponds to $\lambda_1 = -0.3$ GeV^2, and the lower one to the maximal value for λ_1 that can be accommodated in the model (24), $\lambda_1 \sim -0.43$ GeV^2. The solid dots are the nonperturbative corrections according to (19), while the solid triangles are the corrections using the model (24) for the nonperturbative function F.

We have also plotted separately the contributions to the moments originating from the term linear in n of (19) (open circles) and the rest, i.e., the constant terms and terms decreasing with n (open squares).

In both cases, small and large λ_1, one finds a substantial contribution from the chromomagnetic-moment term λ_2, at least for small moments. The term from the kinetic energy operator has a linear dependence on n [cf. (19)] while the chromomagnetic term behaves like a constant for large n. The linear terms of (19) are well reproduced by the model for the nonperturbative function; this is to be expected, since the nonperturbative function contains only the most singular contribution in each order of the $1/m_b$ expansion, i.e., the leading twist term. On the other hand, from the fact that the linear term in n from (19) already approximates the nonperturbative function quite well, one may conclude that the expansion (19) is in fact sufficient for the range of n we are considering. In other words, the leading-twist contribution modeled by the ansatz (24) may be replaced by the term proportional to λ_1/m_b^2 in the $1/m_b$ expansion of the moments with high accuracy. In particular this means that the most singular contribution of order $1/m_b^3$ remains small for the moments we consider.

However, the result (19) differs from what the nonperturbative function gives, mainly because of the

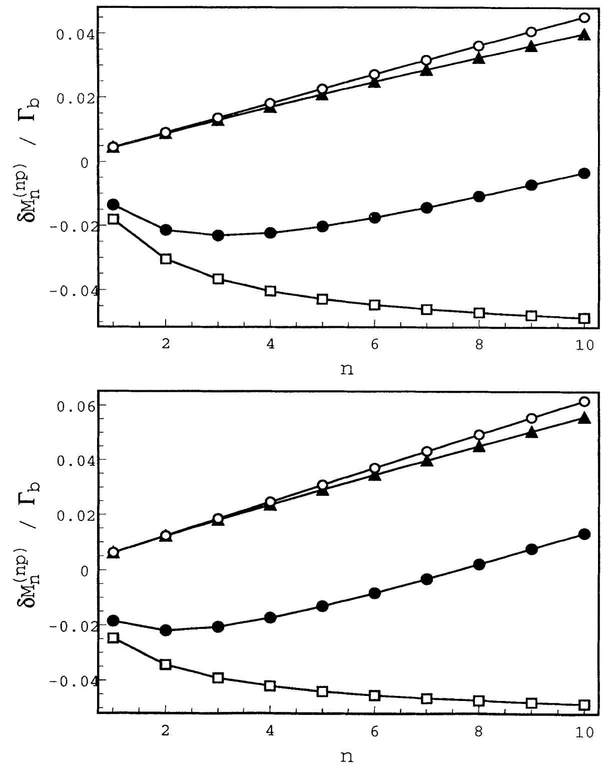

FIG. 2. The nonperturbative corrections to the moments for $\lambda_1 = -0.3$ GeV^2 (upper figure) and $\lambda_1 = -0.43$ GeV^2 (lower figure). The solid dots are the corrections using the lowest nontrivial contributions (19), the solid triangles are the corrections from the nonperturbative function as given in (27), the open circles are the contributions from the $n\lambda_1$ alone in (19), and the open boxes are the contributions except the $n\lambda_1$ term.

chromomagnetic-moment term and the constant terms proportional to λ_1. These terms are less singular than the contribution of $n\lambda_1$, but they contribute substantially to the moments $n < 10$. On the other hand, the leading-twist terms indicate that the $1/m_b$ expansion is satisfactory for $n < 10$ and we conclude that the expansion (19)

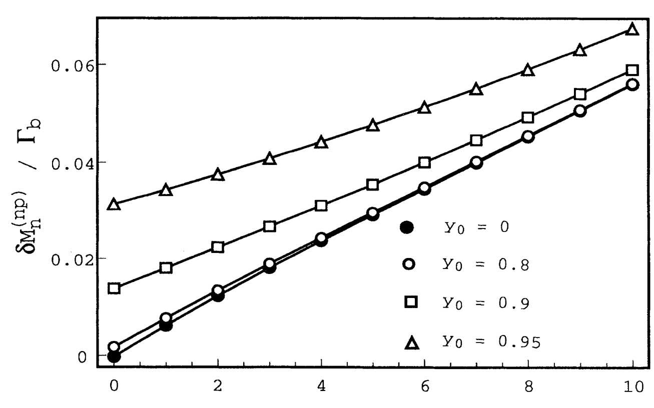

FIG. 3. The nonperturbative corrections to the moments, including a lower cut of y_0 in the integration as in (17). We use $\rho = 0$, corresponding to $\lambda_1 = -0.43$ GeV^2.

is justified for the moments in the range considered.

Finally, one may also consider the effect of a lower cutoff y_0 in the integration over y as in (17). The strongest effects are expected for large λ_1, so we plot in Fig. 3 the nonperturbative corrections for $\rho = 0$ in the model (24), for different values of the cutoff y_0. For the realistic case $y_0 = 0.9$ one finds only small corrections for $4 < n < 10$, and the conclusion concerning the minimal n obtained from the parton model remains valid.

Next we consider the radiative corrections. In Fig. 4 we plot these corrections to the moments $\delta\mathcal{M}_n^{(\mathrm{rc})}$ obtained from the one-loop result (7), from the exponentiation of the leading double logarithms, both for fixed scale $\mu = m_b$ and for variable scale $\mu = m_b(1-y)$. We use in (7) the value of α_s at m_b, $\alpha_s(m_b) = 0.26$, corresponding to $\Lambda_{\mathrm{QCD}} = 250$ MeV.

The radiative-correction contribution to the moments with $n > 4$ is rather stable; in other words, it does not depend on how one deals with the end-point singularities. Compared to the nonperturbative corrections for small λ_1, they are much larger, dominating the corrections to the moments. This smallness of the nonperturbative corrections is due to an almost cancellation between the contributions of λ_1 and λ_2 in the region of n we are considering.

We may also consider the contributions to the moments of a subleading logarithmic contribution. The logarithmic contributions to the spectrum have the general form [18]

$$\frac{d\Gamma}{dy} = \sum_{k=0}^{\infty}\sum_{l=0}^{2k}\left(\frac{\alpha_s}{\pi}\right)^k \ln^{2k-l}(1-y)C_{kl}, \tag{28}$$

where C_{kl} is a set of coefficients. Calculating the moments of (28) for α_s taken at a fixed scale $\mu = m_b$, one obtains

$$\mathcal{M}_n = \sum_{k=0}^{\infty}\sum_{l=0}^{2k}\left(\frac{\alpha_s(m_b^2)}{\pi}\right)^k \Delta(2k-l,n)C_{kl}, \tag{29}$$

where

$$\Delta(l,n) = \int_0^1 dy\, y^n \ln^l(1-y)$$
$$= \sum_{j=0}^{n}\binom{n}{j}(-1)^{j+l}l!\left(\frac{1}{j+1}\right)^{l+1}. \tag{30}$$

The first few $\Delta(l,n)$ are tabulated in Table I. For the region of n we are interested in, the order of magnitude of $\Delta(l,n)$ is determined by the factor $l!$; furthermore they are alternating in sign due to the factor $(-1)^l$. The contribution of the subleading logarithms depends strongly on their (unknown) coefficients C_{kl}; for the leading contribution $l = 2k$ it is known (at least in the Abelian case) that they sum into an exponential as in (7), which means

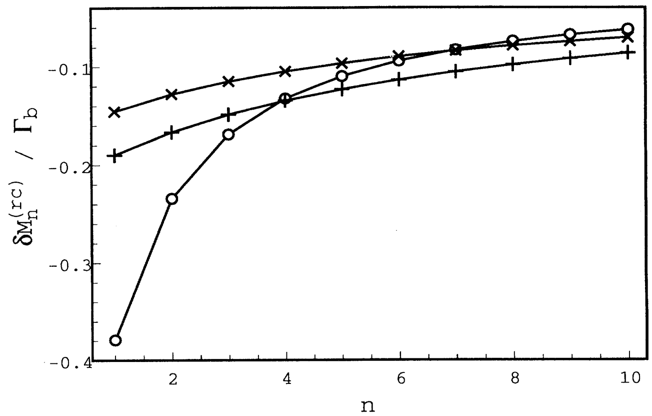

FIG. 4. The radiative corrections to the moments. Open circles correspond to (7) with $\alpha_s(m_b) = 0.26$, the crosses correspond to (9) with $\alpha_s(m_b) = 0.26$, and the $\times$'s are obtained from (11).

that the coefficients C_{kl} have to behave as an inverse factorial

$$C_{k,2k} = (-1)^k 1/k! \tag{31}$$

Still the expansion of the exponential does not commute with the evaluation of the integral for the moments, even for the $\mathcal{M}_0$, the total rate. In other words, the perturbative expansion of the moments for small enough n behaves in a similar way as the one for the total rate, and thus we expect that perturbation theory for the first few moments to be as good as the perturbative expansion for the total rate. A similar conclusion, namely that perturbation theory is applicable to moments with low n, is reached in a recent preprint by Sterman and Korchemskii [22], where radiative corrections to moments defined in a similar way have been considered.

The effect of a lower cut in the y integration for the moments as in (17) leads to a doubly logarithmic dependence of the form $\ln^2(1-y_0)$ on the lower cut y_0; if y_0 comes close to 1, the effects of the lower cut may become large, forcing us to go to higher n. However, numerically it turns out that, with realistic values of y_0, the situation still remains under control. This is shown quantitatively in Fig. 5, where we use expressions (7) (upper figure) and (9) (lower figure) to estimate the effect of a lower bound. Depending on n and on the lower cut y_0 the variation in $\delta\mathcal{M}_n$ may be up to a factor of 2 for small n ($n \sim 4$), but it decreases rapidly for larger n ($n \sim 10$); however, the moment to leading order is still large for small n and the net effect of the cut remains small in the region of interest.

Our main conclusion is thus that one may use the combined expansion for the moments below $n = 10$, which is given by

$$\mathcal{M}_n = \Gamma_b\left[\frac{2}{n+1} + \frac{\lambda_1}{3m_b^2}\left(\frac{10}{n+1} - 1 - n\right) + \frac{\lambda_2}{m_b^2}\left(\frac{22}{n+1} - 11\right)\right.$$
$$\left. - \frac{4\alpha_s(m_b)}{3\pi(n+1)}\left(\frac{5}{4}+\pi^2\right) - \frac{4\alpha_s(m_b)}{3\pi}\left(\Delta(l=2,n) + \frac{31}{6}\Delta(l=1,n)\right)\right] + O\left(\left(\frac{\bar{\Lambda}}{m_b}\right)^3, \alpha_s^2(m_b), \left(\frac{\bar{\Lambda}}{m_b}\right)^2\alpha_s(m_b)\right). \tag{32}$$

TABLE I. Numerical values for the functions $\Delta(l,n)$ for $0 < n < 10$ and $1 < l < 6$.

n	$\Delta(l=6,n)$	$\Delta(l=5,n)$	$\Delta(l=4,n)$	$\Delta(l=3,n)$	$\Delta(l=2,n)$	$\Delta(l=1,n)$
0	720.0	−120.0	24.00	−6.000	2.000	−1.000
1	714.4	−118.1	23.25	−5.625	1.750	−0.750
2	709.1	−116.4	22.60	−5.324	1.574	−0.611
3	704.1	−114.8	22.02	−5.073	1.441	−0.521
4	699.3	−113.4	21.51	−4.860	1.335	−0.457
5	694.8	−112.0	21.04	−4.675	1.249	−0.408
6	690.4	−110.7	20.61	−4.511	1.176	−0.370
7	686.3	−109.5	20.22	−4.365	1.114	−0.340
8	682.3	−108.4	19.85	−4.233	1.060	−0.314
9	678.4	−107.3	19.51	−4.114	1.013	−0.293
10	674.7	−106.3	19.19	−4.005	0.971	−0.274

Furthermore, the fact that data will be available only for $y > y_0 \sim 0.9$ has a small effect on the moments in the range of n considered; the moments including a lower cut y_0 may still be treated in the combined expansion.

The final result for the moments is plotted in Fig. 6, where those obtained from the combined expansion in $\alpha_s(m_b)$ and $\bar{\Lambda}/m_b$ according to (32) are shown. The solid dots are the result for "small" $\lambda_1 = -0.3$ GeV^2, and the solid boxes are for "large" $\lambda_1 = -0.6$ GeV^2.

To summarize, one may analyze the moments up to 12 before the corrections become too big, of order 100%. We also see that nonperturbative corrections are very small for small values of λ_1, and that the key role is played by the radiative ones. The reason for the smallness of nonperturbative corrections is an almost complete cancellation between the terms proportional to λ_1 and λ_2. For the case $\lambda_1 = -0.6$ GeV^2 the cancellation is only partial and the nonperturbative corrections are sizable and positive. This indicates that higher-twist effects may play an important role also in the end-point region, and taking into account only the leading-twist contribution, corresponding to the function F, is not enough. This remark, however, applies to a precise description of the spectrum in the end-point region, while for the moments with sufficiently small n it is safe to use the combined expansion in $\alpha_s(m_b)$ and $\bar{\Lambda}/m_b$, which contains pieces of nonleading twist in the constant terms and the contributions decreasing with n.

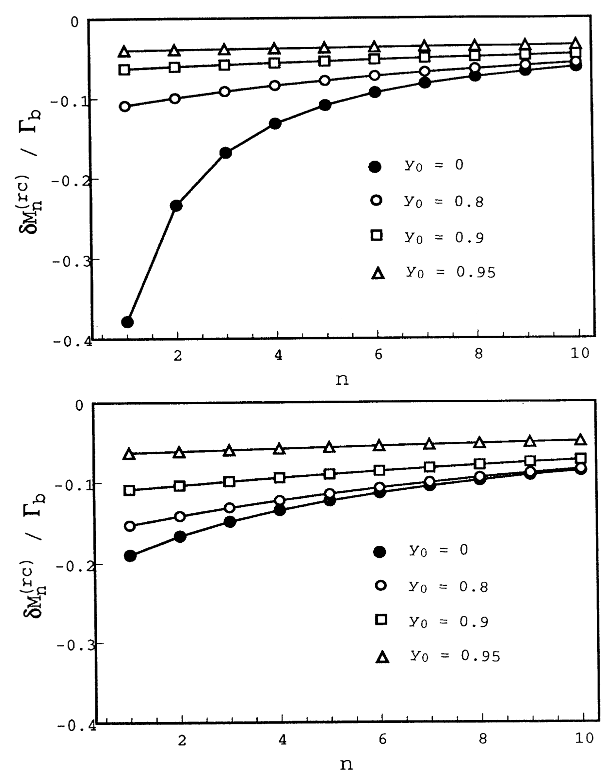

FIG. 5. The effect of a lower cutoff y_0 [cf. (17)] on the radiative corrections to the moments. The upper figure is the moments obtained from (7) with lower cutoff, while the lower plot is obtained from (9).

IV. CONCLUSIONS

Since data on $b \to u$ transitions will be restricted to a small window between 2.3 and 2.6 GeV, it is mainly the end point of the spectrum that will be accessible to experiment. On the other hand, the end-point region is the most difficult region from the theoretical point of

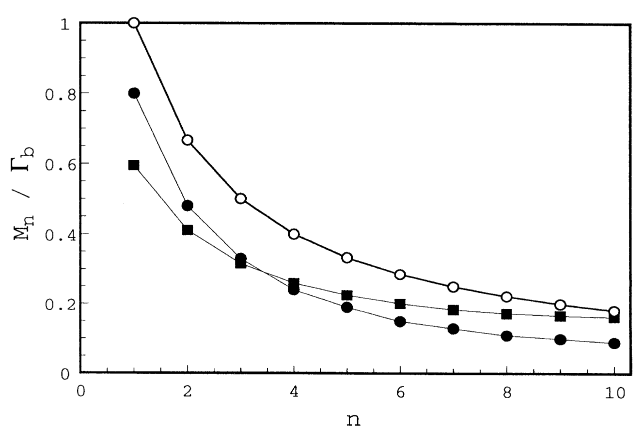

FIG. 6. The final result for the moments, including both radiative and nonperturbative corrections according to (32). The solid dots are the result for $\lambda_1 = -0.3$ GeV^2, the solid boxes are for $\lambda_1 = -0.6$ GeV^2. For comparison we also plot the parton model result (open circles).

view, since here large radiative corrections are entangled with large nonperturbative effects. In fact, it is not even obvious whether and how the two sources of corrections may be distinguished close to the end point.

The main result of this paper is that one may define suitable averages of the inclusive decay distribution of semileptonic $b \to u$ transitions, which, on the one hand, may be calculated reliably, and which, on the other hand, are mainly sensitive in the window between the kinematic end points of $b \to c$ and $b \to u$ semileptonic decays. We have concentrated on moments of the energy spectrum of the charged lepton and have performed a detailed numerical analysis, which shows that moments for $n < 10$ may be systematically calculated in a combined $\alpha_s(m_b)$ and Λ/m_b expansion; both types of corrections may be studied systematically. Furthermore, the moments with $n > 4$ are sensitive mainly in the experimentally accessible window. Thus there is indeed a region $4 < n < 10$ for which the moments defined above may be useful to perform a determination of $|V_{ub}|$.

In fact, such a combined expansion is even valid for moments defined with a lower cutoff y_0, as given in (17) as long as y_0 is not too close to 1. Furthermore, for a realistic value $y_0 = 0.9$ the deviations of the moments including a cut from the full ones are small in the region of n considered. Thus for an experimental analysis one may as well deal with the moments including a cut.

In order to extract $|V_{ub}|$ from these moments one has to know the two matrix elements λ_1 and λ_2. While λ_2 is known from the hadron spectrum, λ_1 is still uncertain; we have used typical "large" and "small" values, but one may hope to extract this parameter from experiment eventually. Furthermore a comparison to the structure function approach shows that the most singular terms of order $1/m_b^3$ and higher remain small for the range of moments under consideration.

One possibility to perform a determination of λ_1 is in fact to use the moments defined above. The ratio of two moments will depend only on λ_1/m_b^2, λ_2/m_b^2 and $\alpha_s(m_b)$. The strong coupling and λ_2 are known, and one may in principle extract λ_1 and m_b from two ratios of moments. After having done this, one may use any one of the moments to obtain Γ_b and hence $|V_{ub}|$. To proceed along these lines one needs a measurement of three moments in the range $4 < n < 10$; any measurement of additional moments may be used to cross-check the n dependence of the moments.

We have discussed how sensitive the moments are to the end-point region. From this point of view, one has to have n as large as possible; the fourth moment receives about 50% from the end-point region ($y > 0.9$), while for $n = 10$ one has already 70% contribution from this region. Using this method to determine V_{cb} the sensitivity to the end-point region translates into an error in this kind of analysis. However, a detailed analysis of the errors is very much connected to the question of how much of the end-point region is accessible in the experiment. The applicability of our method (as well as its error) may then be estimated by comparing the n dependence of the measured moments to the n dependence as predicted in (32). A realistic error of this method is somewhere in the range 20–30 %, if only the end-point region is experimentally accessible and no further (in general model-dependent) assumptions are made.

The idea presented here may be refined in various aspects, and we consider this paper as a first try to study whether one may extract $|V_{ub}|$ using the moments of the decay distributions. As far as the radiative corrections are concerned, we have only considered the singular and nonvanishing terms close to the end point. In this point one may refine the analysis by taking into account the complete corrections, which may be found in the literature. Furthermore, also the corrections of order $(\bar{\Lambda}/m_b)^3$ have been considered [23] and also may be included in the analysis. However, we do not expect that any of these higher-order corrections will change any of our conclusions.

Finally, one may also think of considering other averages of decay distributions and generalize the moments according to

$$\widetilde{\mathcal{M}}_n = \int_0^{1+\bar{\Lambda}/m_b} dy\ \mathcal{F}_n(y)\frac{d\Gamma}{dy}, \tag{33}$$

where $\mathcal{F}_n$ is some set of functions. A good choice of $\mathcal{F}_n$ may possibly allow a more reliable calculation of the corresponding moments $\widetilde{\mathcal{M}}_n$, and, on the other hand, be more sensitive to the experimentally accessible region.

ACKNOWLEDGMENTS

We want to thank the Theory group of SLAC, and especially M. Peskin and S. Brodsky, for the hospitality extended to both of us. It was a pleasure to discuss issues concerning this paper with S. Brodsky, M. Peskin, and H. Anlauf. B.B. also wants to thank M. Shifman, T.M. D. Cassel, M. Neubert, and N. Uraltsev for discussions.

[1] J. Chay, H. Georgi, and B. Grinstein, Phys. Lett. B **247**, 399 (1990).
[2] I. Bigi, N. Uraltsev, and A. Vainshtein, Phys. Lett. B **293**, 430 (1992).
[3] B. Blok and M. Shifman, Nucl. Phys. **B399**, 441 (1993); **399**, 459 (1993).
[4] I. Bigi, B. Blok, M. Shifman, N. Uraltsev, and A. Vainshtein, in *The Fermilab Meeting*, Proceedings of the Meeting of the Division of Particles and Fields of the APS, Batavia, Illinois, 1992, edited by C.H. Albright *et al.* (World Scientific, Singapore, 1993), Vol. 1, p. 610.
[5] I. Bigi, M. Shifman, N. Uraltsev, and A. Vainshtein, Phys. Rev. Lett. **71**, 496 (1993).
[6] B. Blok, L. Koyrakh, M. Shifman, and A. Vainshtein, Phys. Rev. D **49**, 3356 (1994).
[7] A. Manohar and M. Wise, Phys. Rev. D **49**, 1310 (1994).

[8] A. Falk, M. Luke, and M. Savage, Phys. Rev. D **49**, 3367 (1994).
[9] T. Mannel, Nucl. Phys. **B413**, 396 (1994).
[10] M. Neubert, Phys. Rev. D **49**, 3392 (1994); **49**, 4623 (1994).
[11] I. Bigi, M. Shifman, N. Uraltsev, and A. Vainshtein, Int. J. Mod. Phys. A **9**, 2467 (1994).
[12] T. Mannel and M. Neubert, Phys. Rev. D **50**, 2037 (1994).
[13] A. Ali and E. Pietarinen, Nucl. Phys. **B154**, 519 (1979).
[14] N. Cabibbo, G. Corbo, and L. Maiani, Nucl. Phys. **B155**, 93 (1979).
[15] G. Altarelli, N. Cabibbo, G. Corbo, L. Maiani, and G. Martinelli, Nucl. Phys. **B208**, 365 (1982).
[16] G. Corbo, Nucl. Phys. **B212**, 99 (1983).
[17] M. Jezabek and J. H. Kühn, Nucl. Phys. **B320**, 20 (1989).
[18] A. Falk, A. Manohar, E. Jenkins, and M. Wise, Phys. Rev. D **49**, 4553 (1994).
[19] M. Neubert, contribution to "QCD94," Montpellier, France, 1994 (unpublished).
[20] P. Ball and V.M. Braun, Phys. Rev. D **49**, 2472 (1994).
[21] I. Bigi, M. Shifman, N. Uraltsev, and A. Vainshtein, Phys. Lett. B **328**, 431 (1994).
[22] G. Korchemsky and G. Sterman, Phys. Lett. B **340**, 96 (1994).
[23] A specific $1/m_b^3$ contribution has been considered in I. Bigi and N. Uraltsev, Nucl. Phys. **B423**, 33 (1994).